Spectrum-Energy Efficiency Tradeoff of Distributed Antenna Network

Hidetoshi Kaji† Shinya Kumagai† Katsuhiro Temma† and Fumiyuki Adachi‡
Dept. of Communications Engineering, Graduate School of Engineering, Tohoku University
6-6-05 Aza-Aoba, Aramaki, Aoba-ku, Sendai, 980-8579, Japan
†{kaji, kumagai, tenma}@mobile.ecei.tohoku.ac.jp, ‡adachi@ecei.tohoku.ac.jp

***Abstract*—It is well known that the spectrum efficiency (SE) and energy efficiency (EE) of wireless network have a tradeoff relationship. In cellular networks, the same frequency is reused among a number of cells and the frequency reuse factor (FRF) considerably affects the SE-EE tradeoff relationship in terms of the co-channel interference (CCI) and network capacity. In distributed antenna network (DAN), antennas are spatially distributed over the entire coverage area and hence, short-distance communications are allowed, thereby both the EE and SE are improved compared with conventional centralized antenna network (CAN) for the same FRF. In this paper, we derive the tradeoff relationship between SE and EE of DAN taking FRF into account. Numerical results show that FRF=1 maximizes the SE and EE over the entire cell in DAN and that DAN achieves better SE-EE tradeoff relationship than CAN.**

Keywords—distributed antenna network; spectrum efficiency; energy efficiency; frequency reuse

I. INTRODUCTION

Recently, broadband data services have been strongly demanded in wireless networks. However, the required bandwidth and transmit power increase in proportion to the data rate. Therefore, an efficient use of spectrum and energy resources in broadband wireless communications has been a hot topic [1]. It is well known that the spectrum efficiency (SE) and energy efficiency (EE) of wireless network have a tradeoff relationship. In cellular networks, the same frequency is reused among a number of cells and frequency reuse factor (FRF) considerably affects the SE-EE tradeoff relationship.

Broadband wireless channel is characterized by distance-dependent path loss, shadowing loss, and frequency-selective fading [2]. Space diversity technique is a quite powerful technique to mitigate the frequency-selective fading. In conventional cellular network (which is called the centralized antenna network (CAN) in this paper), antennas are co-located at the base station (BS). This is sufficient for mitigating the fading impact. However, the space diversity using co-located antennas cannot mitigate the negative impacts resulting from path and shadowing losses.

In order to simultaneously mitigate the problems arising from the path loss, shadowing loss, and fading, distributed antenna network (DAN) [3], [4] or distributed antenna system (DAS) [5], [6] has recently been attracting much attention. In DAN, antennas are spatially distributed over the entire coverage area and hence, the impacts resulting from path and shadowing losses can be mitigated as well as the fading. It has been shown that DAN allows single frequency reuse and improves the SE compared with CAN [7]. Furthermore, DAN allows short-distance communications (since user can find nearby distributed antennas) and achieves higher received signal power than CAN even with significantly reduced transmit power [8]. Therefore, DAN can achieve higher EE compared with CAN while improving the SE for the same FRF. However, to the best of our knowledge, the impact of FRF on the SE-EE tradeoff in DAN has not been discussed.

In this paper, we derive the SE-EE tradeoff relationship of DAN taking FRF into account and discuss the impact of FRF on SE-EE tradeoff.

The remainder of this paper is organized as follows. In Section II, we define SE and EE. Section III describes the system model of DAN downlink. In Section IV, Monte Carlo numerical results are shown. Section V gives some conclusions.

II. SPECTRUM AND ENERGY EFFICIENCIES DEFINITION

Fig. 1 shows the model of cellular network assumed in this paper. The same frequency is reused in spatially separated cells to utilize the limited frequency bandwidth efficiently [2]. The available frequency bandwidth is divided into N sub-bands, where N is called FRF. Each sub-band is reused in spatially separated different cells. In this paper, the center cell (i=0) is the cell of interest and is surrounded by 6 co-channel interference (CCI) cells in the first tier.

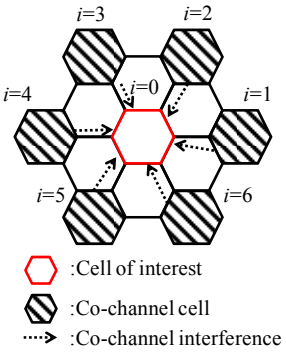

Fig. 1. Celluar network model (e.g. N=3).

A. Spectrum Efficiency (SE)

The SE η_s (bits/sec/Hz/km^2) is defined as

$$\eta_s \equiv \frac{C_{total}}{S_{total} \cdot B_{total}} = \frac{N \cdot C}{(N \cdot S) \cdot (N \cdot B)} = \frac{1}{N \cdot S} \cdot \frac{C}{B}, \quad (1)$$

where C_{total} (bits/sec) and B_{total} (Hz) denote the achievable total capacity and the total bandwidth in the cluster area S_{total} (km^2) of N cells, respectively. B (Hz) is the bandwidth of each sub-band (which is assigned to each cell) and S (km^2) is the cell area. C (bits/sec) is the achievable channel capacity per cell. Letting $c=C/B$ (bits/sec/Hz), η_s can be rewritten as

$$\eta_s = \frac{c}{N \cdot S}. \quad (2)$$

B. Energy Efficiency (EE)

The EE η_e (bits/J) is defined as the number of bits transmitted per Joule and is expressed as

$$\eta_e = \frac{C_{total}}{P_{total}} = \frac{N \cdot C}{N \cdot P_t} = \frac{c}{P_t / B}, \quad (3)$$

where P_{total} (Watt) and P_t (Watt) are the total transmit power radiated in the area S_{total} of N cells consisting of one cluster and in the each cell area, respectively.

C. Relationship between SE and EE

We assume the frequency-domain signal transmission such as OFDM and SC-FDE. The channel capacity c (bits/sec/Hz) is given as [1]

$$c = \frac{1}{N_f} \sum_{k=0}^{N_f-1} \log_2 \left\{ 1 + \frac{P_r(k)}{G(k)} \right\}, \quad (4)$$

where N_f denotes the number of orthogonal subcarriers, and $P_r(k)$ and $G(k)$ denote the instantaneous received signal power and the average CCI plus background noise power on the k(=0~N_f–1)-th subcarrier, respectively. The CCI plus noise can be approximated as a zero-mean additive white Gaussian noise (AWGN) by central limit theorem. Substituting Eq. (4) into Eqs. (2) and (3) gives

$$\eta_s = \frac{1}{N \cdot S} \frac{1}{N_f} \sum_{k=0}^{N_f-1} \log_2 \left\{ 1 + \frac{P_r(k)}{G(k)} \right\}, \quad (5)$$

and

$$\eta_e = \frac{\frac{1}{N_f \cdot N} \sum_{k=0}^{N_f-1} \log_2 \left\{ 1 + \frac{P_r(k)}{G(k)} \right\}}{P_t / B}. \quad (6)$$

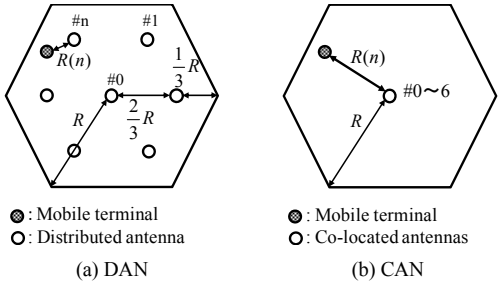

(a) DAN (b) CAN

Fig. 2. Cell model.

Increasing the transmit power P_t increases the received signal power $P_r(k)$, but also increases the CCI plus noise power $G(k)$. Therefore, c increases slowly with P_t. On the other hand, the denominator of the right-hand side of Eq. (6) linearly increases with P_t. As a result, increasing P_t leads to EE degradation. Therefore, η_s and η_e have a tradeoff relationship.

D. Cell Model

Fig. 2 shows the cell model for DAN and CAN. A single mobile terminal (MT) equipped with a single receive antenna is randomly located in each cell. In DAN, 7 antennas are distributed in a cell and are connected with the signal processing center (SPC). In CAN, the BS having 7 co-located antennas is located at the center of a cell.

E. Channel Model

We assume a downlink single-input single-output (SISO) block transmission with cyclic prefix (CP) insertion. The data symbol block of N_c symbols is transmitted by one antenna selected from 7 antennas. Throughout the paper, symbol-spaced discrete time representation is used. The received signal power $P_r^{(i,n)}$ of the user in the cell of interest is expressed as [3]

$$P_r^{(i,n)} = A \cdot P_t^{(i,n)} \cdot \left(R^{(i,n)} \right)^{-\alpha} \cdot 10^{-\frac{\eta^{(i,n)}}{10}}, \; i=0\sim6, \quad (7)$$

where A is a constant including the transmit/receive antenna gains and feeder loss, $P_r^{(i,n)}$ is the transmit power of the n-th antenna in the i-th cell, α is the path loss exponent, and $R^{(i,n)}$ and $\eta^{(i,n)}$ are respectively the shadowing loss in dB and the distance between the n-th antenna in the i-th cell and the user in the cell of interest.

By introducing the normalized distance $r^{(i,n)}=R^{(i,n)}/R$ with R being the cell radius and the normalized transmit power $\widetilde{P}_t^{(i,n)} = A \cdot P_t^{(i,n)} \cdot R^{-\alpha}$, Eq. (7) can be rewritten as

$$P_r^{(i,n)} = \widetilde{P}_t^{(i,n)} \cdot \Omega^{(i,n)}, \quad (8)$$

where $\Omega^{(i,n)} = \left(r^{(i,n)} \right)^{-\alpha} \cdot 10^{-\eta^{(i,n)}/10}$.

By assuming that the frequency-selective channel is composed of L distinct paths, the channel impulse response

$h^{(i,n)}(\tau)$ between the n-th antenna in the i-th cell and the MT in the cell of interest can be represented as

$$h^{(i,n)}(\tau)=\sum_{l=0}^{L-1}h_l^{(i,n)}\delta(\tau-\tau_l^{(i,n)}), \tag{9}$$

where $h_l^{(i,n)}$, $\tau_l^{(i,n)}$, and $\delta(\tau)$ are respectively the complex-valued path gain of the l(=0~L−1)-th path with $E[\sum_{l=0}^{L-1}|h_l^{(i,n)}|^2]=\Omega^{(i,n)}$ ($E[.]$ denotes the ensemble average operation), the delay time of the l-th path, and the delta function. The n'-th antenna having the largest square sum of the path gains (i.e., $n'=\arg\max_{n=0\sim N_t-1}\sum_{l=0}^{L-1}|h_l^{(0,n)}|^2$) is selected for transmission.

F. Channel Capacity

The transmit block consisting of N_c symbols associated with the i-th cell is denoted as $\{d^{(i)}(t);\ t=0\sim N_c-1\}$. The last N_g symbols of each transmit block are copied as a CP and inserted into the guard interval (GI) before transmission.

The time-domain received signal after CP removal at the MT receiver in the 0-th cell of interest is given as

$$\begin{aligned}y^{(0)}(t)=&\sqrt{\frac{2E_s}{T_s}}\sum_{l=0}^{L-1}h_l^{(0,n')}d^{(0)}((t-\tau_l^{(0,n')})\bmod N_c)\\&+\sqrt{\frac{2E_s}{T_s}}\sum_{i=1}^{6}\sum_{l=0}^{L-1}h_l^{(i,n')}d^{(i)}((t-\tau_l^{(i,n')})\bmod N_c)\\&+z^{(0)}(t),\end{aligned} \tag{10}$$

where $E_s=\widetilde{P}_t^{(i,n)}\cdot T_s$ is the normalized transmit symbol energy with T_s being the symbol duration. $\{z^{(0)}(t);\ t=0\sim N_c-1\}$ is a sequence of zero-mean Gaussian noise samples having variance $2N_0/T_s$ with N_0 being the one-sided power spectrum density of AWGN.

The time-domain received signal $\{y^{(0)}(t);\ t=0\sim N_c-1\}$ is transformed by N_c-point discrete Fourier transform (DFT) into the frequency-domain received signal $\{Y^{(0)}(k);\ k=0\sim N_c-1\}$, which is given as

$$Y^{(0)}(k)=\sqrt{\frac{2E_s}{T_s}}H^{(0)}(k)D^{(0)}(k)+I^{(0)}(k)+Z^{(0)}(k), \tag{11}$$

where $H^{(i)}(k)$ is the channel transfer function between the n'-th transmit antenna in the i-th cell and the MT in the cell of interest, $D^{(i)}(k)$ is the frequency-domain transmit signal in the i-th cell, $I^{(0)}(k)$ is the CCI component, and $Z^{(0)}(k)$ is the noise component, which are given as

$$\begin{cases}H^{(i)}(k)=\sum_{l=0}^{L-1}h_l^{(i,n')}\exp(-j2\pi kl/N_c)\\D^{(i)}(k)=\frac{1}{\sqrt{N_c}}\sum_{t=0}^{N_c-1}d^{(i)}(t)\exp(-j2\pi kt/N_c)\\I^{(0)}(k)=\sqrt{\frac{2E_s}{T_s}}\sum_{i=1}^{6}H^{(i)}(k)D^{(i)}(k)\\Z^{(0)}(k)=\frac{1}{\sqrt{N_c}}\sum_{t=0}^{N_c-1}z^{(0)}(t)\exp(-j2\pi kt/N_c)\end{cases}. \tag{12}$$

In this paper, $I^{(0)}(k)$ is assumed to be a zero-mean complex Gaussian variable. Therefore, $I^{(0)}(k)+Z^{(0)}(k)$ becomes a new zero-mean complex Gaussian variable.

The instantaneous received signal power, $P_r(k)$, and the average CCI plus background noise power, $G(k)$, on the k(=0~N_c−1)-th subcarrier are expressed as

$$P_r(k)=\frac{2E_s}{T_s}\left|H^{(0)}(k)\right|^2, \tag{13}$$

$$G(k)=E\left[\left|I^{(0)}(k)+Z^{(0)}(k)\right|^2\right], \tag{14}$$

where $E[|I^{(0)}(k)|^2]$ is given as

$$\begin{aligned}&E[|I^{(0)}(k)|^2]\\&=E\left[\sum_{i=1}^{6}\frac{2E_s}{T_s}H^{(i)}(k)D^{(i)}(k)\left\{H^{(i)}(k)D^{(i)}(k)\right\}^*\right]\\&=\frac{2E_s}{T_s}\sum_{i=1}^{6}\left|H^{(i)}(k)\right|^2.\end{aligned} \tag{15}$$

Substituting Eq. (15) into Eq. (14), we have

$$G(k)=\frac{2E_s}{T_s}\sum_{i=1}^{6}\left|H^{(i)}(k)\right|^2+\frac{2N_0}{T_s}. \tag{16}$$

As a consequence, the channel capacity c (bits/sec/Hz) is given as

$$\begin{aligned}c&=\frac{1}{N_c}\sum_{k=0}^{N_c-1}\log_2\left\{1+\frac{P_r(k)}{G(k)}\right\}\\&=\frac{1}{N_c}\sum_{k=0}^{N_c-1}\log_2\left\{1+\frac{\frac{E_s}{N_0}\left|H^{(0)}(k)\right|^2}{1+\frac{E_s}{N_0}\sum_{i=1}^{6}\left|H^{(i)}(k)\right|^2}\right\},\end{aligned} \tag{17}$$

where E_s/N_0 denotes the normalized transmit symbol energy-to-AWGN power spectrum density.

G. Normalized SE and EE

In this paper, we introduce the following normalized SE $\hat{\eta}_s$ and EE $\hat{\eta}_e$. They are given as

$$\hat{\eta}_s = S \cdot \eta_s = \frac{c}{N}, \tag{18}$$

$$\hat{\eta}_e = \left(A \cdot R^{-\alpha} \cdot \frac{B}{N_0 / T_s} \right)^{-1} \cdot \eta_e = \frac{1}{N} \frac{c}{\left(\frac{E_s}{N_0} \right)} = \frac{\hat{\eta}_s}{\left(\frac{E_s}{N_0} \right)}. \tag{19}$$

By using the normalized SE and EE, the SE and EE relationship can be discussed for a given cell radius R.

III. Numerical Evaluation

The downlink SE and EE assuming one communicating user per cell are evaluated by Monte Carlo numerical computation method using Eqs. (18) and (19). The location of a MT is randomly generated in a cell (see Fig. 2). The cell radius R is used as the reference distance. The cumulative distribution functions (CDFs) of SE and EE are measured. In this paper, the outage SE (EE) is introduced; the x%-outage SE (EE) is defined as the one which the SE (EE) falls below with probability of x%. The numerical computation condition is summarized in Table I.

TABLE I. Numerical Evaluation Condition

Path loss exponent	α=3.0
Shadowing	Log-normal with standard deviation σ=7.0(dB)
Fading type	Frequency-selective block Rayleigh
Number of paths	L=16
Power delay profile	Symbol-spaced uniform
DFT size	N_c=128

A. Outage SE

Fig. 3 plots the 10%-outage SE in DAN as a function of normalized transmit E_s/N_0 with FRF N as a parameter. For comparison, 10%-outage SE in CAN is also plotted. DAN always achieves higher 10%-outage SE than CAN irrespective of value of N. It is also seen from Fig. 3 that N=1 always maximizes the 10%-outage SE in DAN irrespective of the normalized transmit E_s/N_0. DAN allows short-distance communications and accordingly, can improve the received signal-to-interference plus noise power ratio (SINR) without increasing N; this leads to the fact that N=1 maximizes the 10%-outage SE. On the other hand, in CAN, N=3 or 4 is found to maximize the 10%-outage SE when the normalized transmit E_s/N_0>4dB while N=1 maximizes the 10%-outage SE when the normalized transmit E_s/N_0<0dB. For high normalized transmit E_s/N_0's, the CCI is a predominant factor to determine the SE. Therefore, increasing N makes the distance between user and co-channel cells longer and consequently, reduces the CCI, thereby improving the SE. However, too much increase of N leads to reduced sub-bandwidth assigned to each cell, thereby reducing the SE.

Fig. 4 plots the 90%-outage SE in DAN as a function of normalized transmit E_s/N_0 with FRF N as a parameter. For comparison, 90%-outage SE of CAN is also plotted. Fig. 4 shows that N=1 maximizes the 90%-outage SE for both CAN and DAN. 90%-outage SE represents the SE associated with the user located close to the transmit antenna (where the channel capacity limiting factor is not the CCI but the noise).

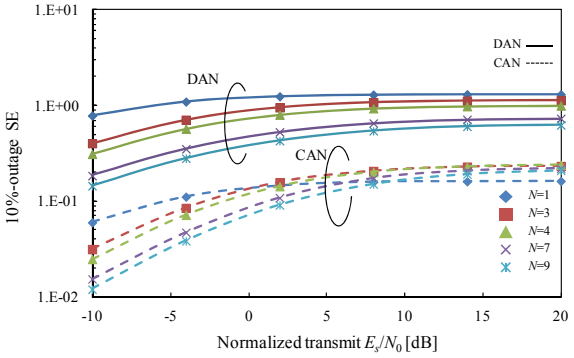

Fig. 3. 10%-outage SE.

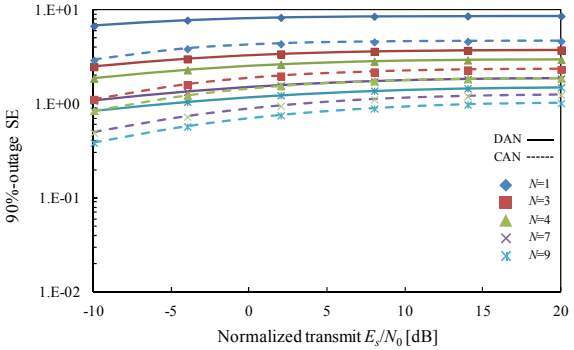

Fig. 4. 90%-outage SE.

B. Outage EE

Fig. 5 plots the 10%-outage EE in DAN as a function of normalized transmit E_s/N_0 with FRF N as a parameter. For comparison, 10%-outage EE in CAN is also plotted. It can be seen from Fig. 5 that 10%-outage EE in DAN is maximized when N=1. This is because DAN can reduce the transmit power significantly and accordingly reduce CCI sufficiently without increasing FRF N. For CAN, similar to the result of SE, N=3 or 4 is found to maximize the 10%-outage EE for the normalized transmit E_s/N_0>4dB while N=1 maximizes the 10%-outage EE for normalized transmit E_s/N_0<0dB.

Fig. 6 plots the 90%-outage EE in DAN as a function of the normalized transmit E_s/N_0 with FRF N as a parameter. For comparison, 90%-outage EE in CAN is also plotted. N=1 is found to maximize the 90%-outage EE both in CAN and DAN. The 90%-outage EE represents the EE associated with the MT located close to the transmit antenna, where the channel capacity limiting factor is not the CCI but the noise. Therefore,

the channel capacity increases only logarithmically with the increase in the transmit power, thereby N=1 maximizes the 90%-outage EE and increasing the normalized transmit E_s/N_0 decreases the 90%-outage EE.

C. SE-EE Tradeoff

Fig. 7 plots the 10%-outage SE-EE tradeoff in DAN with FRF N as a parameter for various values of the normalized transmit E_s/N_0. For comparison, the 10%-outage SE-EE tradeoff in CAN is also plotted. It can be seen from Fig. 7 that DAN has better SE-EE tradeoff than CAN. This is because the communication distance in DAN is much shorter and the same SE is obtained with much lower transmit E_s/N_0.

Fig. 8 plots the 90%-outage SE-EE tradeoff in DAN with FRF N as a parameter for various values of the normalized transmit E_s/N_0. The 90%-outage SE-EE tradeoff in CAN is also plotted. It can be seen from Fig. 8, the tradeoff curves of CAN are close to those of DAN. The 90%-outage SE-EE tradeoff in CAN is associated with the user located close to the cell center and the channel capacity limiting factor is the noise. Therefore, CAN with collocated antennas provides a good SE-EE tradeoff. However, DAN can still provide better SE-EE tradeoff than CAN.

IV. CONCLUSIONS

In this paper, we derived the SE-EE tradeoff relationship taking FRF into account. Numerical results showed that FRF=1 maximizes the SE and EE over the entire cell in DAN and that DAN achieves a much better SE-EE tradeoff relationship than CAN. Extension to multiple-input multiple-output (MIMO) case is left as an interesting future study.

REFERENCES

[1] Y. Chen, S. Zhang, and S. Xu, "Fundamental trade-offs on green wireless networks," *IEEE Commun. Mag.*, vol.49, no.6, pp.30-37, June 2011.

[2] A. Goldsmith, *Wireless communication*, Cambridge University Press, 2005.

[3] F. Adachi, K. Takeda, T. Yamamoto, R. Matsukawa, and S. kumagai, "Recent advances in single-carrier distributed antenna network," *Wireless Communications and Mobile Computing*, vol.11, no.12, pp.1551-1563, Dec. 2011. DOI: 10.1002/wcm.1212.

[4] F. Adachi, W. Peng, T. Obara, T. Yamamoto, R. Matsukawa, and M. Nakada, "Distributed antenna network for gigabit wireless access," *International Jounal of Electronics and Communications (AEUE)*, vol.66, no.8, pp.605-612, Aug. 2012.

[5] W. Feng, Y.Li, S. Zhou, J. Wang and M. Xia, "Downlink capacity of distributed antenna systems in a multi-cell environment," *in Proc. 2009 IEEE Wireless Communications and Networking Conference (WCNC2009)*, Nudapest, Hungary, Apr. 2009.

[6] H. Hu, Y. Zhang, and Y. Yao, *Distributed antenna systems*; *open architecture for future wireless communications*, Auerbach Pub., 2007.

[7] S. Kumagai, R. Matsukawa, T. Obara, T. Yamamoto and F. Adachi, "Spectral efficiency of distributeds antenna network using MIMO spatial multiplexing," *in Proc. 76th IEEE Vehicular Technology Conference (VTC2012-Fall)*, Quebec, Canada, Sept. 2012.

[8] R. Matsukawa, T. Obara, K. Takeda, and F. Adachi, "Downlink throughput performance of distributed antenna network using tranmit/receive diversity," *in Proc IEEE 74th Vehicular Technology Conference (VTC2011-Fall)*, CA, USA, Sept. 2011.

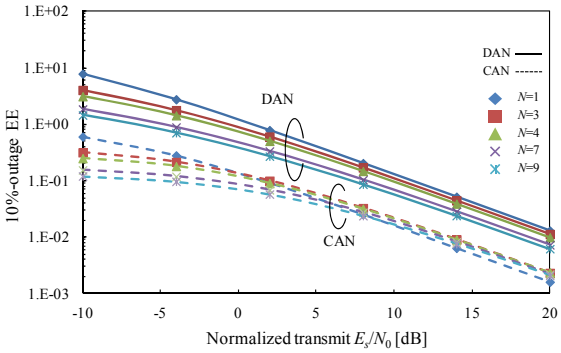

Fig. 5. 10%-outage EE.

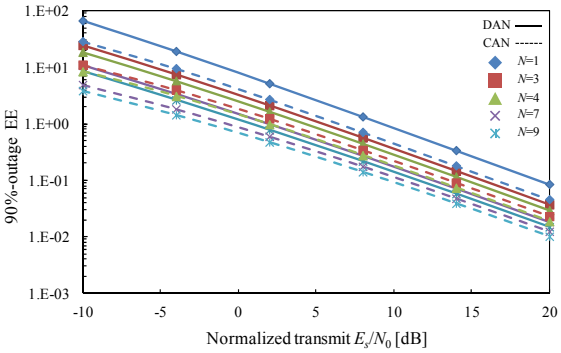

Fig. 6. 90%-outage EE.

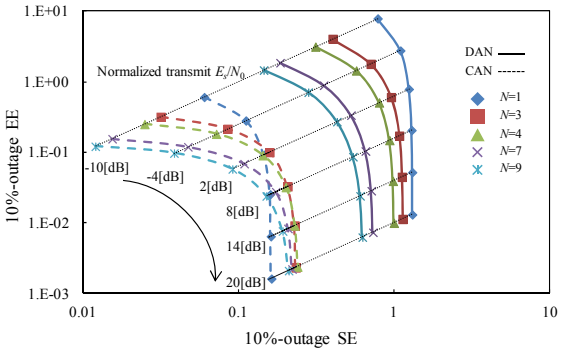

Fig. 7. Tradeoff between 10%-outage SE and EE.

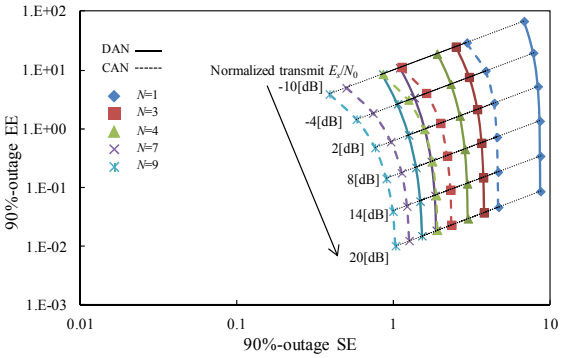

Fig. 8. Tradeoff between 90%-outage SE and EE.